

**Orographic Precipitation in Potentially
Unstable Alpine Storms:
MAP IOPs 2b, 3, and 5**

**Socorro Medina and Robert A. Houze, Jr.
Atmospheric Sciences, University of
Washington, Seattle, USA**

**Preprints, [ICAM/MAP Meeting](#), Brig,
Switzerland, 19-23 May.**

See Following Pages

Orographic Precipitation in Potentially Unstable Alpine Storms: MAP IOPs 2b, 3, and 5

Socorro Medina and Robert A. Houze, Jr.

Atmospheric Sciences, University of Washington, Seattle, USA

1. Introduction

Many intense autumn Alpine storms occur ahead of strong baroclinic troughs. This pattern is commonly associated with large precipitation amounts over the southern Alpine slopes since it tends to produce flow with southerly component around 850 mb, i.e. flow perpendicular to the terrain (Massacand et al. 1998). MAP-SOP IOP2b occurred under this synoptic pattern, exhibiting precipitation amounts of more than 250 mm over the western slopes of the Lago Maggiore (LM) area. Medina and Houze (2003) analyzed IOP2b and proposed a conceptual model of the mechanisms that must have accounted for the enhancement of precipitation that occurred on the lower windward slopes of the Alps. They suggested that the weak moist stability of the air approaching the Alps allowed the flow to rise easily and suddenly over the first major rise of terrain. In addition to this rapid rise, the release of the potential instability of the flow produced overturning and caused precipitation particles over the first major peak of terrain to grow rapidly and fallout, thus making the orographic precipitation enhancement very efficient (Smith 1979). The purpose of this paper is to test this conceptual model by determining if similar precipitation mechanisms occurred in IOPs 3 and 5, which also had air of slight potential instability approaching the Alpine barrier.

2. Review of IOP2b

Medina and Houze (2003) found that in IOP2b the atmosphere was potentially unstable below ~ 700 mb. A Milan sounding taken at 1200 UTC 20 September 1999 showed that the equivalent potential temperature decreased from the surface up to ~ 700 mb, except in a thin stable layer centered around 800 mb (Fig. 1, solid line). The NCAR S-Pol polarimetric radar showed the detailed precipitation and airflow structures. Figure 2a-c shows a vertical cross section of mean S-Pol radar data during IOP2b (1300 UTC 19 September - 0100 UTC 21 September 1999) in the direction approximately parallel to the low-level wind. The radial velocity exhibited a jet rising abruptly over the first peak of the terrain (Fig. 2a). Thus, the entire layer of the atmosphere rose over the Alpine barrier, efficiently advecting and condensing low-level moisture. A low-altitude precipitation maximum formed over the first peak of the terrain, suggesting that raindrops grew by coalescence (Fig. 2b), probably in the manner suggested by Neiman et al. (2002). In addition, Medina and Houze (2003) found evidence that riming growth occurred above the 0°C level, further promoting the rapid growth and fallout of precipitation on the lower windward slopes. This result was obtained by applying particle identification algorithms to the polarimetric radar data (Vivekanandan et al. 1999). Contours of frequency of occurrence of identified particle types show that graupel tended to occur above the first peak of the terrain, directly above the low-level reflectivity maximum and at the exit of the radial velocity jet (Fig. 2c). The vertically pointing OPRA radar (Yuter and Houze 2003) showed updrafts > 2 m/s, suggesting that the existing potential instability was released when the air was lifted over the mountains, and that convective cells were triggered. With simple model calculations Yuter and Houze (2003) showed that these cells further enhanced the growth of particles by coalescence and riming. Thus, the orographic precipitation enhancement in IOP2b was seen to be the result of air with slight potential instability rising rapidly and forming embedded convective cells over the first sharp rise in the terrain.

3. Other potentially unstable cases: IOPs 3 and 5

MAP-SOP IOPs 3 and 5, like IOP2b, occurred ahead of baroclinic troughs. According to a Milan sounding taken at 0000 UTC 26 September 1999 during IOP3 the atmosphere was potentially unstable from ~ 975 to 700 mb (Fig. 1, dashed line). The mixing ratio and temperature of IOP3 below ~ 800 mb were very similar to the values observed in IOP2b (not shown). A cross section of S-Pol radar data

in a direction approximately parallel to the low-level wind and intersecting the Alps shows that during IOP3 (1500 UTC 25 September - 1500 UTC 26 September) the radial velocity had a low-level jet rising over the first peak of the terrain (Fig. 2d), very similar to the jet seen in IOP2b (Fig. 2a). The reflectivity cross section is also consistent with what was observed during IOP2b (Fig. 2e), i.e. there was a stratiform background of precipitation with a low-level cellular maximum over the first peak of the terrain, suggestive of coalescence growth. The polarimetric radar data expressed as the frequency of occurrence of particles accumulated during IOP3 indicated the occurrence of graupel associated with the first steep rise of the terrain (Fig. 2f).

For IOP5, a sounding taken at Milan at 1200 UTC 3 October 1999 exhibited potential instability from the surface to 800 mb (Fig. 1, dash dotted line) as did both IOPs 2b and 3. However, this case had a considerably lower mixing ratio below 850 mb than the previous IOPs and a higher LCL than IOP2b. An IOP5 S-Pol radar cross section parallel to the wind and intersecting the Alps (2000 UTC 02 October - 1600 03 October 1999 mean) is shown in Fig. 2g-i. The patterns of reflectivity and frequency of occurrence of microphysical particles (Fig. 2h and i, respectively) were similar to those of IOPs 2b and 3. However, in IOP5 the radial velocity did not show a sloping jet but a weak horizontal jet above the first of the terrain (Fig. 2g).

4. Conclusions

The stability, airflow and precipitation structures seen during IOP3 were comparable to those of IOP2b. In IOP5, the airflow pattern showed a less pronounced radial velocity jet. In all three cases, the radar reflectivity exhibited a cellular structure with maximum reflectivity at low levels over the first major peak of the terrain, suggesting coalescence growth at low levels, and the S-Pol radar indicated graupel directly over the low level maximum of reflectivity, indicating that these three IOPs all exhibited a similar pattern of precipitation enhancement by cellular coalescence and riming over the first major peak of the terrain. These results suggest that the conceptual model of precipitation enhancement in this type of storm proposed by Medina and Houze (2003) applies generally to weak potentially unstable flows associated with baroclinic systems passing over the Alps.

ACKNOWLEDGMENTS: This work was supported by National Science Foundation Grant ATM-0221843.

LITERATURE

Neiman, P. J., F. M. Ralph, A. B. White, D. E. Kingsmill, and P. O. G. Persson, 2002: The statistical relationship between upslope flow and rainfall in California's coastal mountains: Observations during CALJET. *Mon. Wea. Rev.*, **130**, 1468–1492.

Massacand, A. C., H. Wernli, and H. C. Davies, 1998: Heavy precipitation on the Alpine southside: An upper-level precursor. *Geophys. Res. Lett.* **25**, 1435–1438.

Medina, S. and R. A. Houze, Jr., 2003: Air motions and precipitation growth in Alpine storms. *Quart. J. R. Met. Soc.*, special MAP issue, **129**, 345–371.

Vivekanandan, J., D. S. Zrnić, S. M. Ellis, R. Oye, A. V. Ryzhkov, and J. Straka, 1999: Cloud microphysics retrieval using S-band dual-polarization radar measurements. *Bull. Amer. Meteor. Soc.*, **80**, 381–388.

Yuter, S. E., and R. A. Houze, Jr., 2003: Microphysical modes of precipitation growth determined by S-band vertically pointing radar in orographic precipitation during MAP. *Quart. J. R. Met. Soc.*, special MAP issue, **129**, 455–476.

Smith, R. B., 1979: The influence of mountains on the atmosphere. *Advances in Geophysics*, **21**, Academic Press, 87–230.

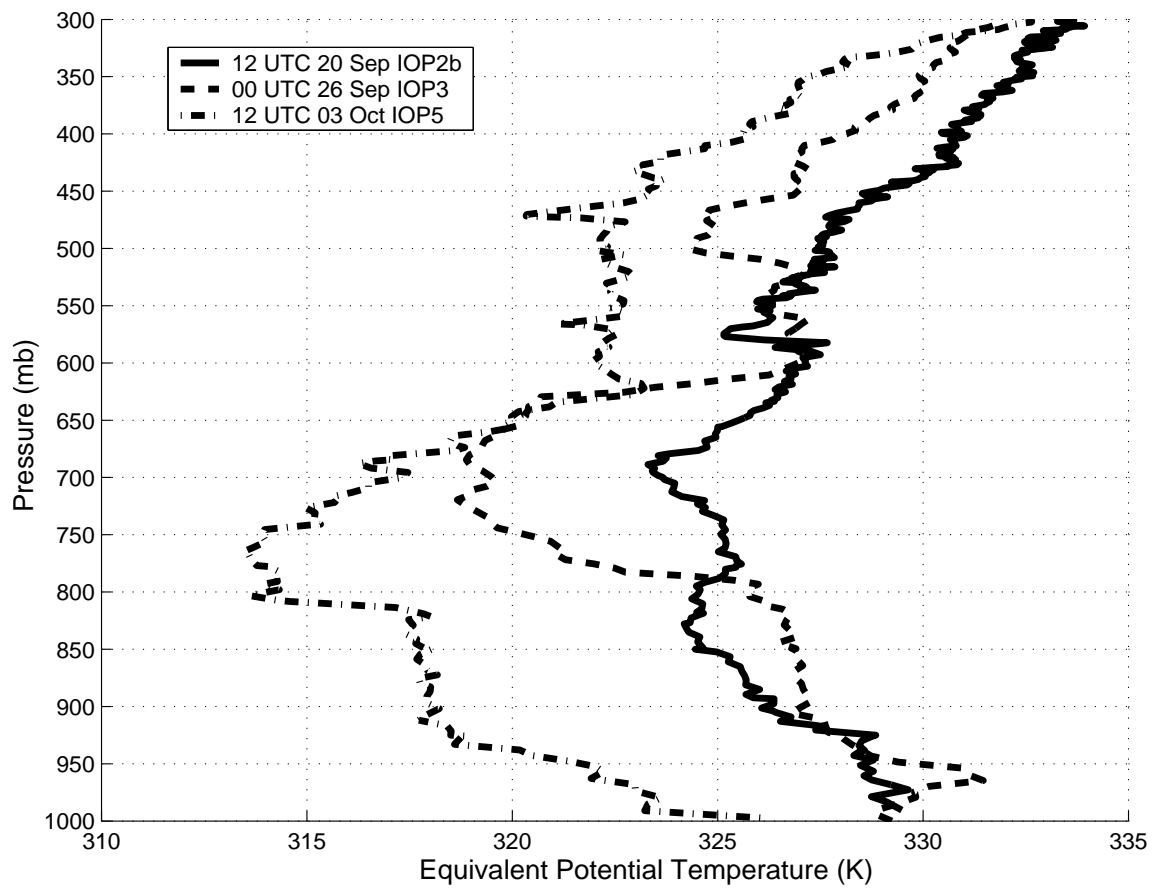


Figure 1: Equivalent potential temperature profiles calculated from Milan soundings taken at 1200 UTC 20 September 1999 during IOP2b (solid line), 0000 UTC 26 September 1999 during IOP3 (dashed line), and 1200 UTC 3 October 1999 during IOP5 (dash dotted line).

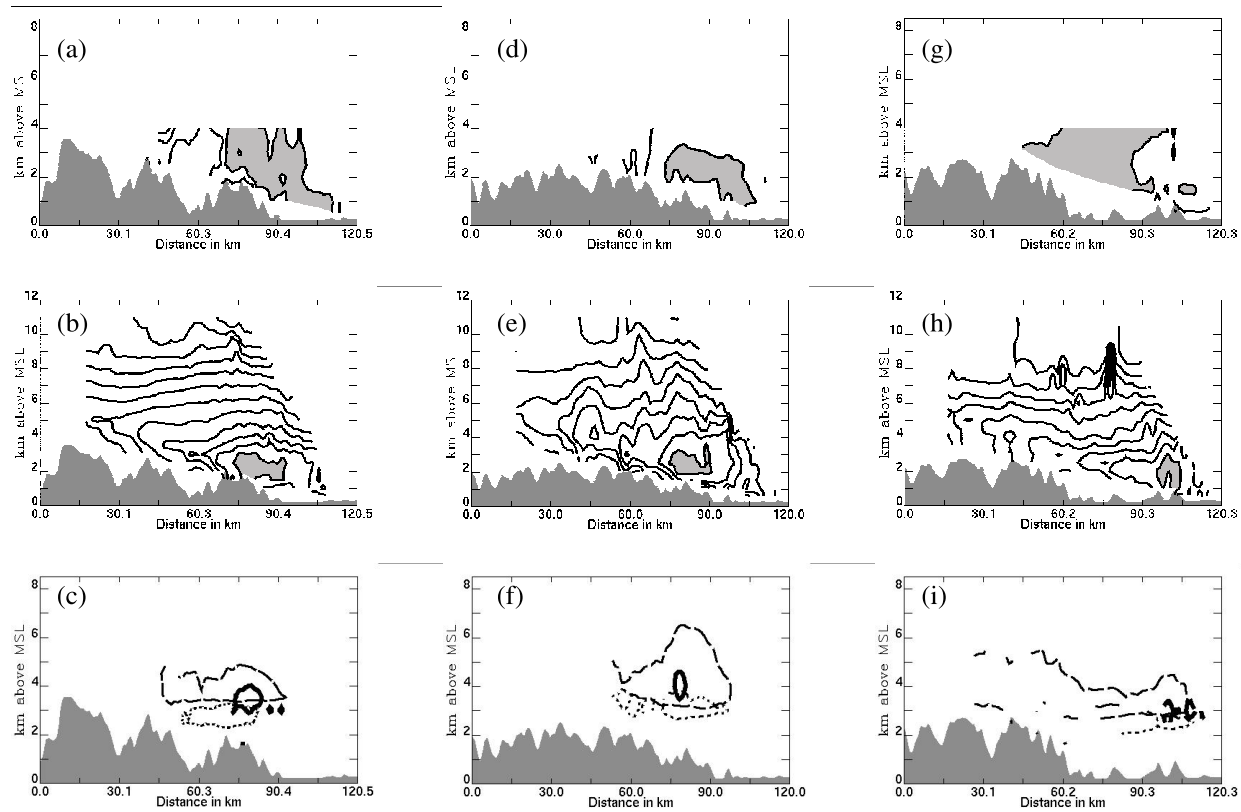


Figure 2: Vertical cross sections of NCAR S-Pol radar data extending from the radar site, located on the lower right corner of the panels, across the Alps to the (a)-(c) north-northwest, (d)-(f) north-northwest, (g)-(i) north. The fields in the panels have been either accumulated or averaged during (a)-(c) IOP2b, (d)-(f) IOP3, and (g)-(i) IOP5. (a) Mean radial velocity contoured every 3 m/s, values between 12-15 m/s shaded. (b) Mean reflectivity contoured every 5 dBZ, values ≥ 36 dBZ shaded. (c) Frequency of occurrence of particle types: 0.5 contour of dry snow (long-dashed), 0.3 contour of wet snow (short dashed), and 0.02 contour of graupel (solid). (d) Mean radial velocity contoured every 3 m/s, values ≥ 9 m/s shaded. (e) Mean reflectivity contoured every 7 dBZ, values ≥ 34 dBZ shaded. (f) Frequency of occurrence of particle types: 0.1 contour of dry snow (long-dashed), 0.03 contour of wet snow (short dashed), and 0.017 contour of graupel (solid). (g) Mean radial velocity contoured every 3 m/s, values between 9-12 m/s shaded. (h) Mean reflectivity contoured every 6 dBZ, values ≥ 32 dBZ shaded. (i) Frequency of occurrence of particle types: 0.1 contour of dry snow (long-dashed), 0.05 contour of wet snow (short dashed), and 0.005 contour of graupel (solid).